Size-Dependent Amorphization of Nanoscale Y_2O_3 at High Pressure

Lin Wang,[1,2,*] Wenge Yang,[1,3] Yang Ding,[1] Yang Ren,[4] Siguo Xiao,[5] Bingbing Liu,[2] Stanislav V. Sinogeikin,[3] Yue Meng,[3] David J. Gosztola,[6] Guoyin Shen,[3] Russell J. Hemley,[7] Wendy L. Mao,[8,9] and Ho-kwang Mao[1,3,7]

[1]*HPSynC, Carnegie Institution of Washington, 9700 South Cass Avenue, Argonne, Illinois 60439, USA*
[2]*State Key Laboratory of Superhard Materials, Jilin University, Changchun 130012, China*
[3]*HPCAT, Carnegie Institution of Washington, 9700 South Cass Avenue, Argonne, Illinois 60439, USA*
[4]*Advanced Photon Source, Argonne National Laboratory, Argonne, Illinois 60439, USA*
[5]*Institute for Nanophysics and Rare Earth Luminescence, Xiangtan University, Xiangtan, 411105, China*
[6]*Center for Nanoscale Materials, Argonne National Laboratory, Argonne, Illinois 60439, USA*
[7]*Geophysical Laboratory, Carnegie Institution of Washington, Washington, D.C. 20015, USA*
[8]*Geological and Environmental Sciences, Stanford University, Stanford, California 94305-2115, USA*
[9]*Photon Science and Stanford Institute for Materials and Energy Sciences, SLAC National Accelerator Laboratory, Menlo Park, California 94025, USA*

(Received 13 April 2010; revised manuscript received 29 July 2010; published 24 August 2010)

Y_2O_3 with particle sizes ranging from 5 nm to 1 μm were studied at high pressure using x-ray diffraction and Raman spectroscopy techniques. Nanometer-sized Y_2O_3 particles are shown to be more stable than their bulk counterparts, and a grain size-dependent crystalline-amorphous transition was discovered in these materials. High-energy atomic pair distribution function measurements reveal that the amorphization is associated with the breakdown of the long-rang order of the YO_6 octahedra, while the nearest-neighbor edge-shared octahedral linkages are preserved.

DOI: 10.1103/PhysRevLett.105.095701 PACS numbers: 64.60.Cn, 61.05.cp, 61.46.Hk, 62.50.−p

The mechanical properties and transformations of nanomaterials under pressure have generated significant interest due to the appearance of size effects on compressional behavior [1–5]. The size effects in nanomaterials are reflected in compressibility transition pressures, and even phase transition routines [2–7]. Determining the critical size which marks the onset of nanoscale effects is one of the crucial parameters required for understanding nanomaterials properties. The critical size depends on many factors including crystal structure, chemical bonding, and phonon instability, etc. For example, significant size effects have been observed at the 100 nm length scale in fullerenes [6,8], whereas they are manifested at ~6 nm for TiO_2 [3,4].

Y_2O_3 is an important industrial compound widely used in many fields [9,10]. The phase stability of Y_2O_3 directly affects its applications. High-pressure optical spectroscopy and x-ray diffraction have been used to study the phase stability of bulk Y_2O_3 [11–13]. The material undergoes two phase transitions on compression and decompression, from cubic to hexagonal and monoclinic phases [13]. Nanoscale Y_2O_3 has potential applications as display material with higher resolution [10,14,15]. 20 nm Y_2O_3 particles were found to exhibit different luminescent properties under pressure, as compared to the bulk [14]. Raman measurements on 60 nm-sized Y_2O_3 nanocrystals have been interpreted from a crystalline to a partially amorphous state at 19 GPa that is not observed in bulk Y_2O_3 [15]. Additional information, including direct measurements of structural properties, is needed to establish such a transition and to identify the mechanism, and the implications for high-pressure behavior of nanoscale materials in general.

Pressure-induced amorphization of oxide materials was first observed for SiO_2 [16,17]. This class of transition has been observed in a broad range of bulk materials [18–20]. A variety of mechanisms, many of which are interrelated, have been proposed to understand these transitions [17]. Here we demonstrate the existence of pressure-induced size-dependent amorphization in nanoscale Y_2O_3 with *in situ* x-ray diffraction, pair distribution analysis, and Raman spectroscopy. The results identify the critical size dependence of the transition. The ambient condition cubic phase transforms to an amorphous form at 24.8 GPa in the 16 nm-sized material, in contrast to 21 nm-sized Y_2O_3 which remains cubic up to 14 GPa after which it transforms to the higher pressure hexagonal phase observed in bulk Y_2O_3. Furthermore, high-energy pair distribution function (PDF) measurements reveal that the amorphization is associated with a breakdown of octahedra connectivity.

The grain size and structure of the starting materials were characterized by dark field transmission electron microscopy (TEM, Philips CM30T) and conventional x-ray diffraction (XRD) methods. High-pressure experiments were conducted with He and silicone oil as pressure-transmitting media, as well as without a medium. Pressure was determined from standard ruby fluorescence techniques [21]. High-pressure XRD and PDF measurements were carried out at 16-IDB and 16-BMD stations, respectively, of the High-Pressure Collaborative Access Team (HPCAT), Advanced Photon Source, Argonne National

Laboratory. Raman spectra of the pristine and recovered samples were measured using a Raman microscope (Renishaw, UK) with 514.5 nm laser excitation.

The crystal structures of the pristine samples of different particle sizes were characterized at ambient conditions by x-ray diffraction. The particle sizes were estimated from the Scherrer equation. Figure 1(a) shows a typical XRD pattern and its refinement for Y_2O_3 with average grain size of 16 nm. The structure of the sample is identified as a cubic structure with space group Ia3 (#206), which is the same as bulk Y_2O_3 [13]. Our results also show that all of the samples of different grain sizes between 5 and 33 nm have the same crystal structure at ambient conditions. Dark field TEM verified the sample particle sizes. The grain sizes obtained from the two methods are consistent [Fig. 1(b)], and a significant lattice expansion can be observed with decreasing particle size [Fig. 1(c)].

XRD patterns of 16 and 21 nm-sized Y_2O_3 at different pressures were obtained (Fig. 2). The diffraction patterns for the 16 nm-sized material indicate that the cubic phase remains to 24.8 GPa, ~12 GPa higher than the transition pressure of the bulk, demonstrating increased stability of the cubic phase in nanoscale Y_2O_3. Above 24.8 GPa, structural disorder sets in, as evidenced by a broad peak appearing at a 2θ of ~7.7°, as well as the gradual disappearance of other diffraction peaks. Above 30 GPa, all diffraction peaks disappear, except for one broad, amorphous peak between 6° and 9°. This indicates that the sample has completely transformed into an amorphous state; XRD of the recovered sample indicates the amorphization is irreversible. On the other hand, the 21 nm material has a distinctly different transition pressure. The cubic phase of this material remains stable up to 14 GPa, at which new peaks associated with hexagonal symmetry are observed at a 2θ of 7.1°, 7.7°, and 8.2° [Fig. 1(b)]. The intensity of the new diffraction peaks increases with pressure and the transition is complete at 32.7 GPa. The hexagonal phase transforms into a monoclinic structure during decompression.

The phase transition of micron-sized Y_2O_3 was also studied for comparison. The result is the same as previously report [13]. The cubic structure transformed into the hexagonal structure at 12 GPa, and the hexagonal structure persists up to the highest studied pressure. From the comparison of the three samples, cubic structured Y_2O_3 shows clear size-dependent stability. The stability increases with decreasing particle size. Most interesting, the pressure-induced amorphization of Y_2O_3 is also size-dependent,

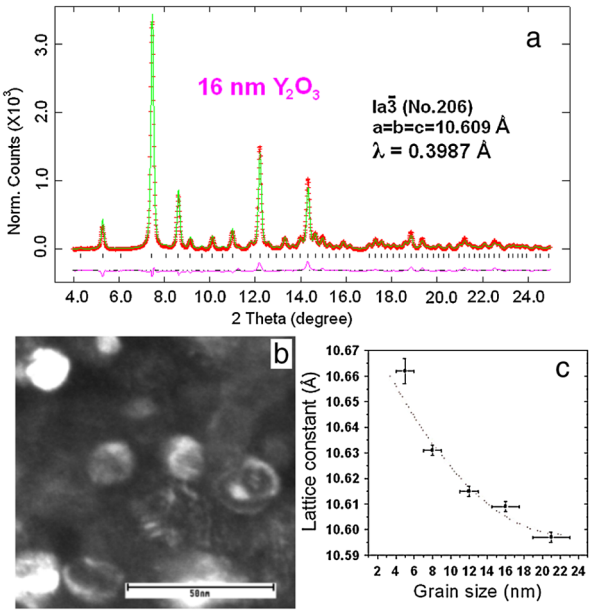

FIG. 1 (color online). (a) Powder x-ray diffraction structure refinement of 16 nm-sized Y_2O_3; (cross: measured pattern; line: calculated pattern; black tick: position of peaks; line below tick: difference between calculated and measured patterns). (b) Dark field TEM image of Y_2O_3 with average particle size of 16 nm. (c) Lattice parameter as a function of particle size.

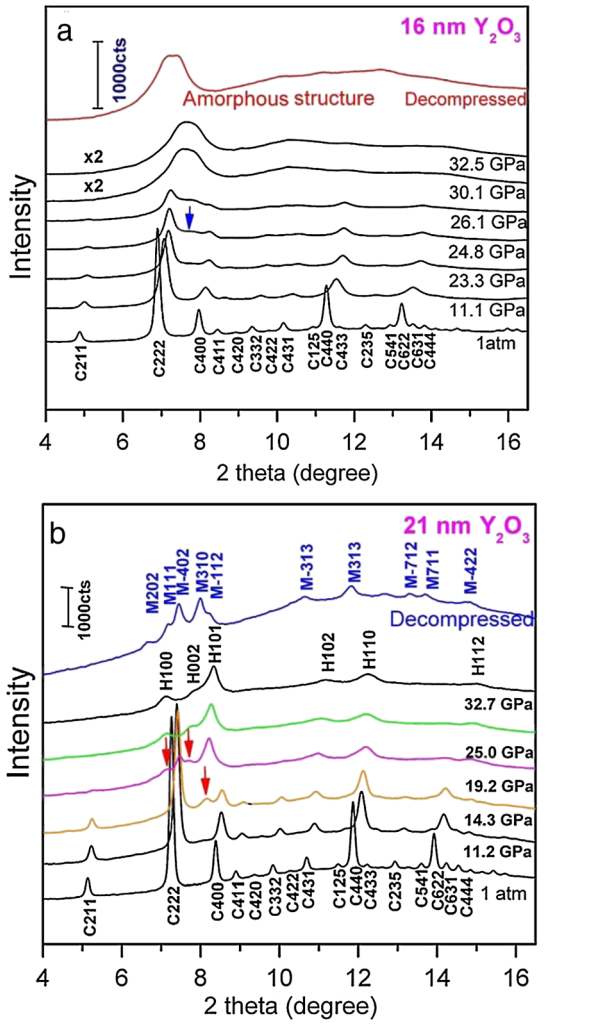

FIG. 2 (color online). (a) X-ray diffraction patterns of 16 nm Y_2O_3 as a function of pressure, $\lambda = 0.3691$ Å. A broad peak at $2\theta \sim 7.7°$ and the gradual disappearance of the other diffraction peaks begin at ~24 GPa and disappear by 32.7 GPa. (b) Patterns for 21 nm-sized Y_2O_3, $\lambda = 0.3875$ Å. The new peaks at 2θ of 6.82° and 7.85° are indicated by red arrows.

and the critical size is in the range of 16–21 nm. Y_2O_3 nanocrystals larger than a critical size behave like the bulk material, whereas the smaller ones transform into an amorphous instead of a crystalline state.

In order to examine the effects of possible pressure inhomogeneity on the transformation, hydrostatic compression, using helium as a medium, and nonhydrostatic compression, without any medium, were used on both 16 and 21 nm-sized Y_2O_3 [Fig. 3(a)]. The 21 nm-sized Y_2O_3 transformed into a hexagonal structure under nonhydrostatic conditions, whereas the 16 nm-sized Y_2O_3 transformed into an amorphous state on hydrostatic compression. The pressure-induced amorphization was confirmed by the Raman measurements on the pressure-released samples. Figure 3(b) shows the comparison of the Raman spectra of pristine 16 nm Y_2O_3 and the Y_2O_3 decompressed from 28 GPa. The Raman spectrum of the pristine material shows several sharp peaks of the lattice vibrations, which indicates that the material is in crystalline structure [15]. However, no peaks can be observed in the Raman spectrum even with much longer collection time for the decompressed sample. This confirms the occurrence of pressure-induced amorphization in the sample.

Size-dependent properties in nanoscale materials under pressure have been shown to include compressibility and crystalline phase stability, but size-dependent amorphization effects have received much less attention (e.g., TiO_2 [3,4]). Solid-state amorphization for many systems can be understood in terms of the lowering of free energies of a high density amorphous phase relative to a metastable lower density crystalline phase [17,22]. Further, the crystalline-amorphous phase transition occurs when $G_a < G_c + G_d$, where G_a is the free energy of the amorphous phase, G_c is the free energy of the metastable crystalline phase, and G_d is the free energy increase due to the presence of defects [23]. In nanoscale crystals, the number of defects associated with the grain boundaries is much larger than in bulk crystals due to the larger volume fraction of grain boundaries. Furthermore, the grain boundary fraction increases with decreasing particle size. For example, the surface fractions of the 16 and 21 nm Y_2O_3 [the thickness of ~1.5(5) nm] estimated from the dark field TEM and XRD measurements are 46% and 37%, respectively. Therefore, the Y_2O_3 nanoscale crystals with smaller grain size have higher G_d. Below a certain critical particle size, G_d becomes large enough to enable $G_a < G_c + G_d$, which triggers amorphization in the nanoscale material. This observation is consistent with previous work which has established that kinetic factors and stability limits also play a role in driving transitions in bulk materials (e.g., Ref. [17]). The finding of a size-dependent transition in octahedrally coordinated nanocrystalline Y_2O_3 is an important new development in understanding the general phenomenon of pressure-induced amorphization.

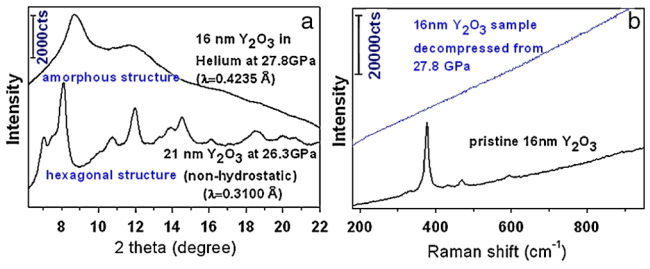

FIG. 3 (color online). (a) XRD patterns of 16 and 21 nm material in different pressure media under compression. (b) Raman spectra of pristine and pressure-released 16 nm Y_2O_3. The excitation laser wavelength was 514.5 nm.

The cubic to hexagonal transition is well understood, but amorphization behavior of nanoscale Y_2O_3 remains unexplored. In order to understand the mechanism of the pressure-induced amorphization from the point of view of the local structure, high-pressure PDF measurement of 16 nm-sized Y_2O_3 was carried out up to 29 GPa [Fig. 4(a)]. For the PDF spectrum at relatively low pressures, all of the well resolved peaks are indexed. The position of each peak represents the distance between each pair of atoms [Fig. 4(b)]. Specifically, the position of the Y-O peak represents the distance between the yttrium and the nearest oxygen. The positions of the Y-Y peaks represent the distances between nearest [*a*-*b* in Fig. 4(c)], second nearest (*a*-*c*) and further Y and Y atoms. The shift of the Y-O peak is very small, which indicates that the Y-O bonding is rigid. The cubic Y_2O_3 phase consists of YO_6 octahedra, in which each Y atom is surrounded by six O atoms. In the measurements, all of the peaks persist up to ~24 GPa, at which point peaks corresponding to distances larger than 3.5 Å start to disappear. By ~29 GPa only two peaks representing the distance between the atoms in each octahedron and between the nearest octahedra remain, and they persist to higher pressures. This observation indicates that each octahedra and the relationship between the two nearest octahedra are preserved after amorphization, but long-range ordering of the octahedra has broken down. The pressure of this change coincides with that of amorphization, consistent with high-pressure-induced amorphization being associated with the disordering of Y_2O_3 octahedra on compression.

Since the YO_6 octahedra are less compressible than the overall Y_2O_3 crystal, the volume compression is mainly achieved by bending the polyhedra-linking angles at the shared corners and edges. For Y_2O_3 with large grain size ($\geq$21 nm), the cubic phase transforms to hexagonal phase at 14 GPa. However, the size-effect stabilizes the cubic phase of Y_2O_3 with smaller grain size at higher pressure, as evinced by the *in situ* high-pressure x-ray diffraction measurements. The cubic phase could survive at higher pressure region without transforming to the hexagonal phase, and the linkage angles continued to bend. Eventually, the structure collapses and transforms into amorphous state, once the bending exceeds its critical limit. This mechanism has also been used to explain the pressure-induced amorphization occurring in many other polyhedra-linked bulk materials (e.g., SiO_2 [17]) when the crystalline-crystalline

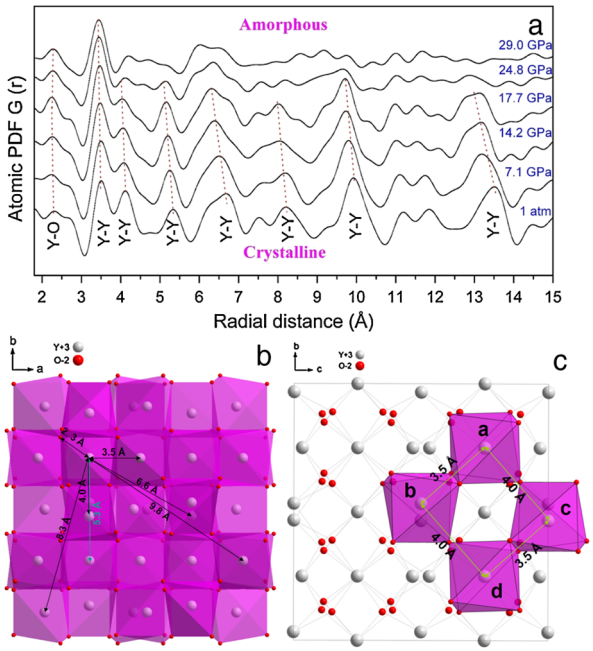

FIG. 4 (color online). (a) Pair distribution function (PDF) of 16 nm-sized Y_2O_3 at different pressures. The x-ray energy was 39.995 keV. Dashed lines are guides for the eye. (b) The structure model for the cubic structure of Y_2O_3. The distances between different atoms are shown with arrows, which correspond to each peak shown in (a). (c) Connections between the nearest octahedra. There is an unoccupied space among the six octahedra (inner and outer ones are not shown).

transition is prohibited while the network structure is compressed and distorted beyond its mechanical limit.

The structure of cubic Y_2O_3 provides further insight into the transition. The space between the six octahedra in the structure is more easily compressed by bending the links than the octahedra themselves [Fig. 4(c)], but ultimately the interstitial space collapses is limited by the cost of breaking bonds. The nearest octahedra (*a*-*b*) are connected with one edge (sharing two oxygen atoms), and the second nearest octahedra (*a*-*c*) are connected with one corner (sharing one oxygen atom). From an energetic point of view, breaking the connection between *a* and *c* is much easier than between *a* and *b*. The coherence between *a* and *c* breaks at the critical pressure, but that between *a* and *b* remains intact, as evidenced by the PDF changes. The extent to which this change is also associated with an elastic instability (e.g., Ref. [17]) remains to be determined.

In conclusion, we have demonstrated a critical size dependence for pressure-induced amorphization of a nanomaterial. Cubic structure in 16 nm-sized Y_2O_3 can be stable up to 24.8 GPa, which is much higher than for bulk Y_2O_3. The cubic phase transformed into an amorphous state at this pressure, whereas bulk Y_2O_3 remains stable in a crystalline structure. Pair distribution function analysis reveals that the breakdown of connectivity between YO_6 octahedra is associated with the amorphization. The variation in pressure-induced polymorphism as a function of particle size found here, including the striking effect on amorphization, reveals the important role that particle size can play in the behavior of materials under extreme conditions.

We thank R. E. Cook, R. Koritala, and O. Shebanova for experimental help, and anonymous reviewers for comments. The research was supported by NSF (MRI-0821584 and EAR-0810255), and the International Balzan Foundation. HPSynC is supported as part of EFree, an Energy Frontier Research Center funded by the U.S. Department of Energy (DOE), Office of Science, Office of Basic Energy Sciences (BES) under Grant Number DE-SC0001057. HPCAT is supported by CIW, CDAC, UNLV and LLNL through funding from DOE-NNSA, DOE-BES and NSF. The work was conducted at the APS, the Electron Microscopy Center for Materials Research, and the Center for Nanoscale Materials at ANL (Contract No. DE-AC02-06CH11357). This work was also partially supported by the NSFC (10979001), the National Basic Research Program of China (2005CB724400).

*wanglin@aps.anl.gov

[1] J. Schiøtz, F. D. D. Tolla, and K. W. Jacobsen, Nature (London) **391**, 561 (1998).
[2] Q. F. Gu *et al.*, Phys. Rev. Lett. **100**, 045502 (2008).
[3] V. Pischedda *et al.*, Phys. Rev. Lett. **96**, 035509 (2006).
[4] V. Swamy *et al.*, Phys. Rev. Lett. **96**, 135702 (2006).
[5] Q. X. Guo *et al.*, Nano Lett. **8**, 972 (2008).
[6] L. Wang *et al.*, Appl. Phys. Lett. **91**, 103112 (2007).
[7] Y. J. Wang *et al.*, Nano Lett. **8**, 2891 (2008).
[8] L. Wang *et al.*, Adv. Mater. **18**, 1883 (2006).
[9] C. B. Willingham *et al.*, *Proc. SPIE 5078 (Window and Dome Technologies VIII)* (2003) p. 179.
[10] T. Igarashi *et al.*, Appl. Phys. Lett. **76**, 1549 (2000).
[11] E. Husson *et al.*, Mater. Res. Bull. **34**, 2085 (1999).
[12] T. Atou *et al.*, J. Solid State Chem. **89**, 378 (1990).
[13] L. Wang *et al.*, Appl. Phys. Lett. **94**, 061921 (2009).
[14] X. Bai *et al.*, J. Nanosci. Nanotechnol. **8**, 1404 (2008).
[15] N. Dilawar *et al.*, Nanotechnology **19**, 115703 (2008).
[16] R. J. Hemley, in *High-Pressure Research in Mineral Physics*, edited by M. H. Manghnani and Y. Syono (Terra Sci., Tokyo/AGU, Washington, D.C., 1987), p. 347.
[17] R. J. Hemley *et al.*, Nature (London) **334**, 52 (1988).
[18] P. Richet and P. Gillet, Eur. J. Mineral. **9**, 907 (1997).
[19] J. Z. Zhang *et al.*, Chem. Mater. **17**, 2817 (2005).
[20] J. S. Tse and D. D. Klug, Phys. Rev. Lett. **70**, 174 (1993).
[21] H. K. Mao, J. A. Xu, and P. M. Bell, J. Geophys. Res. **91**, 4673 (1986).
[22] J. Z. Jiang *et al.*, Europhys. Lett. **50**, 48 (2000).
[23] W. L. Gong *et al.*, Phys. Rev. B **54**, 3800 (1996).